Supplementary information

Facile fabrication of high-density two-dimensional micronozzle arrays using twisted thin-wire molds

Koki Takahashi[a], and Kyohei Terao*[ab]

[a] Department of Intelligent Mechanical Systems Engineering, Kagawa University, Takamatsu 761-0396, Japan. E-mail: terao.kyohei@kagawa-u.ac.jp; Tel: +81 (87) 864-2346

[b] Nano-Micro Structure Device Integrated Research Center, Kagawa University, Takamatsu 761-0396, Japan.

Skewing thin-wire arrays

The spatial positions of the thin-wire array were calculated in a normalized Cartesian coordinate system $(0 \le x,y,z \le 1)$, where the wire lines are initially aligned in parallel between two planes located at $z = 0$ and $z = 1$. The plane at $z = 1$ is rotated by an angle $\theta(0^\circ \le \theta \le 180^\circ)$ with respect to the plane at $z = 0$, while the wire endpoints remain rigidly anchored to the corresponding positions on each plane.

A single wire is defined by two endpoints. Point A is fixed at $(x_0,y_0,0)$ on the plane at $z = 0$, whereas point B, initially located at $(x_0,y_0,1)$, is rotated to point B' at $(x_0',y_0',1)$ on the rotated plane. The position of the wire at an intermediate axial position z, denoted as (x, y), is given by linear interpolation between the two endpoints as

$$\begin{pmatrix} x \\ y \end{pmatrix} = \begin{pmatrix} x_0 \\ y_0 \end{pmatrix} + z\begin{pmatrix} x_0' - x_0 \\ y_0' - y_0 \end{pmatrix}. \qquad \text{(S1)}$$

The rotated coordinates (x_0',y_0') are obtained by applying a two-dimensional rotation matrix to the original coordinates (x_0,y_0):

$$\begin{pmatrix} x_0' \\ y_0' \end{pmatrix} = \begin{pmatrix} \cos\theta & -\sin\theta \\ \sin\theta & \cos\theta \end{pmatrix}\begin{pmatrix} x_0 \\ y_0 \end{pmatrix}. \qquad \text{(S2)}$$

Substituting Eq. (S2) into Eq. (S1), the wire position at any axial coordinate z is expressed as

$$\begin{pmatrix} x \\ y \end{pmatrix} = \begin{pmatrix} 1 - z + z\cos\theta & -z\sin\theta \\ z\sin\theta & 1 - z + z\cos\theta \end{pmatrix}\begin{pmatrix} x_0 \\ y_0 \end{pmatrix}. \qquad \text{(S3)}$$

Using Eq. (S3), the three-dimensional positions of all wires in the array were calculated using MATLAB (MathWorks). Representative results are shown in Fig. S1, illustrating the evolution of the wire configuration as a function of the rotation angle θ. The lower panel highlights the wire positions at the mid-plane ($z = 0.5$), where the lateral spacing between adjacent wires reaches a minimum and wire density is maximized.

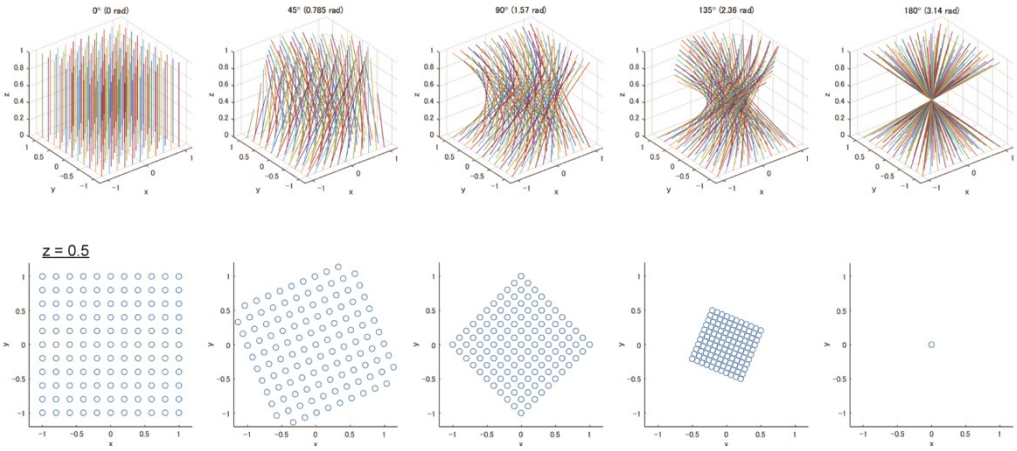

Fig. S1. Calculated configuration of the twisted thin-wire array. (Upper) Three-dimensional wire trajectories for rotation angles ranging from 0° to 180°. (Lower) Cross-sectional positions of the wires at the mid-plane ($z = 0.5$), where maximum wire concentration occurs.

Fabrication setup

The experimental setup for molding and sectioning is shown in Fig. S2. For visualization of wire trajectories during the molding process, nylon wires embedded in polydimethylsiloxane (PDMS) were used as a representative example. All alignment, molding, and sectioning components were fabricated using stereolithography-based 3D printing (Form3, formlab).

Thin wires were manually threaded through a pair of wire-fixing plate jigs (Fig. S3). Each plate contained a triangular hole array that defined the two-dimensional arrangement of the micronozzle array. To prevent physical interference between adjacent wires at the plane of maximum concentration, the hole pattern on one plate was slightly rotated relative to the other, corresponding to a rotation angle of $\theta = 177.5^\circ$. This intentional offset enabled high wire density while maintaining a finite gap between neighboring wires at the concentrated plane.

The wire-fixing plates and threaded wires were assembled into a molding jig (Fig. S4) and secured using four fixation plate jigs, which defined the axial separation and rotational alignment between the plates. The pitch of the wire-fixing holes and the spacing between the plate jigs were set to 9.0 mm and 116 mm for PDMS devices, and 3.0 mm and 50 mm for Ecoflex devices, respectively. The wire-fixing jigs were examined using a digital microscope (Dino-Lite). The distances between adjacent wire-fixing holes were measured at 25 locations for each jig, and measurements were performed for four jigs to determine the mean pitch and standard deviation. After assembly, uncured elastomer was poured into the mold. The entire jig assembly was then mounted within an outer frame jig, in which a spring was attached to apply a constant tensile force to the wire. This tension minimized wire displacement during elastomer curing, particularly in the presence of curing-induced shrinkage.

Following curing, the jig components were removed, and the sacrificial wire was extracted. The cured elastomer block was subsequently sectioned at the plane of maximum wire concentration using a dedicated sectioning jig and a razor blade. The blade was guided along the vertical wall of the jig to ensure reproducible positioning and perpendicular cutting relative to the device surface.

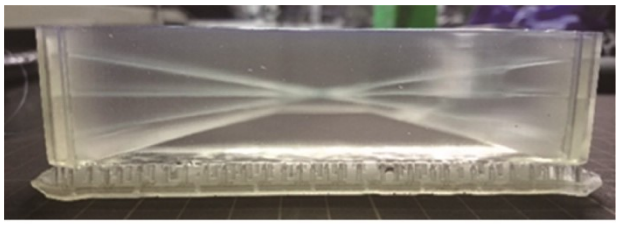

1. Immersed in PDMS

2. Remove jigs and nylon thread

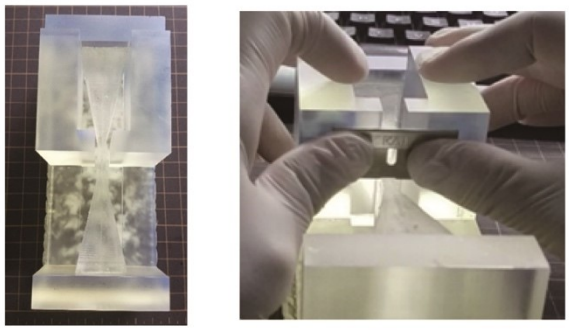

3. Setting and cutting PDMS

Fig. S2. Molding and sectioning process of a micronozzle array device using a nylon wire and PDMS. 1. PDMS resin is poured into the assembled molding jig containing the twisted wire configuration. 2. After curing, the jig components and sacrificial wire are removed from the elastomer block. 3. The PDMS block is sectioned at the plane of maximum wire concentration using a sectioning jig and a razor blade. The blade is guided along the jig wall to cut the block at the narrowest plane in a reproducible manner.

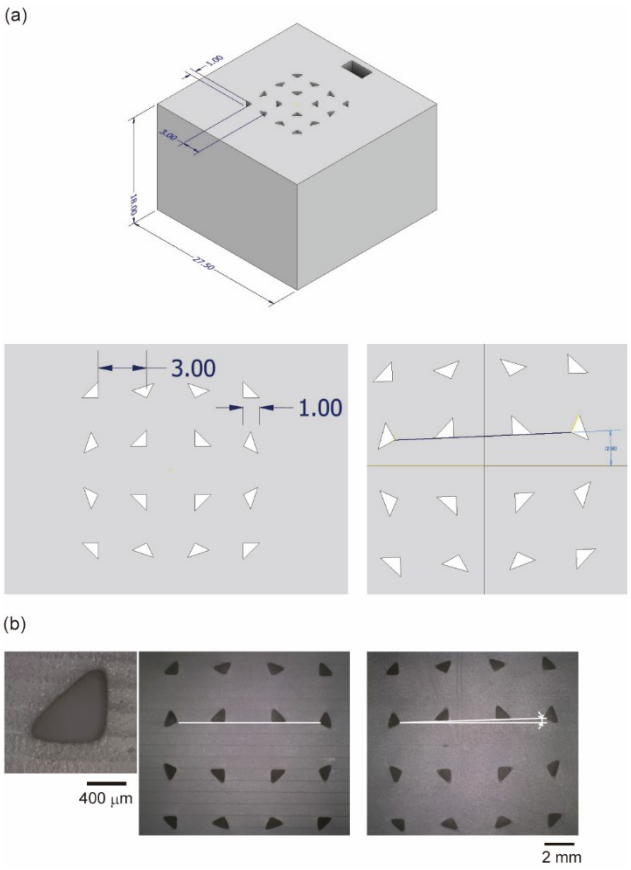

Fig. S3. Wire-fixing plate jigs with triangular hole patterns (4 × 4) designed for a thin piano wire (unit: mm). (a) The hole arrangement defines the two-dimensional layout of the micronozzle array. To avoid physical interference between wires at the concentrated plane, the hole positions on one plate are slightly rotated relative to those on the opposing plate, corresponding to a rotation angle of $\theta = 177.5^\circ$. (b) Photograph of the fabricated wire-fixing jig for 30 μm-diameter piano wires. Right: magnified view of a single triangular anchoring hole. Center and left: images of the 4 × 4 hole array. The right plate includes a 2.5° angular offset relative to the opposing plate (tilt indicated by white guide lines).

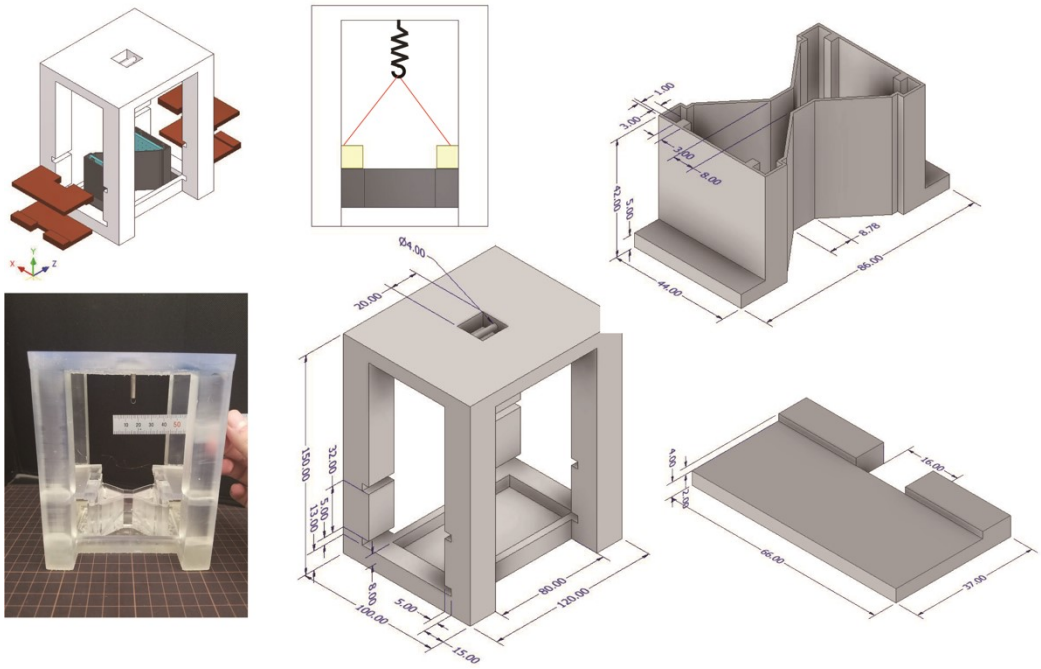

Fig. S4. Dimensions and configuration of the jigs used for piano wire molding (unit: mm). The setup consists of an outer frame jig, a molding and axial-separation jig, and four fixation plate jigs. The outer frame incorporates a spring attachment to apply tensile force to the wire during molding, thereby reducing wire displacement caused by elastomer curing and shrinkage.

Deformation of a thin wire

When polydimethylsiloxane (PDMS) was used as the molding material, deformation of the embedded thin wires was observed after curing (Fig. S5). This deformation is attributed to the relatively large volumetric shrinkage of PDMS during the curing process, which generates internal stresses within the elastomer and induces lateral displacement of the sacrificial wires.

As a result, the spatial arrangement of the wires deviated from the intended geometry at the plane of maximum wire concentration. This deviation led to misalignment of the resulting micronozzle apertures after wire removal and sectioning, as shown in Fig. S5 (right). Although application of tensile force to the wires reduced displacement to some extent, the remaining deformation was sufficient to compromise positional accuracy for high-density micronozzle arrays.

Based on these observations, PDMS was deemed unsuitable for fabricating micronozzle arrays with small aperture diameters and tight spacing using the present twisted thin-wire molding approach. Consequently, a low-shrinkage

silicone elastomer was employed in subsequent experiments to improve wire stability during curing and to achieve reproducible nozzle alignment.

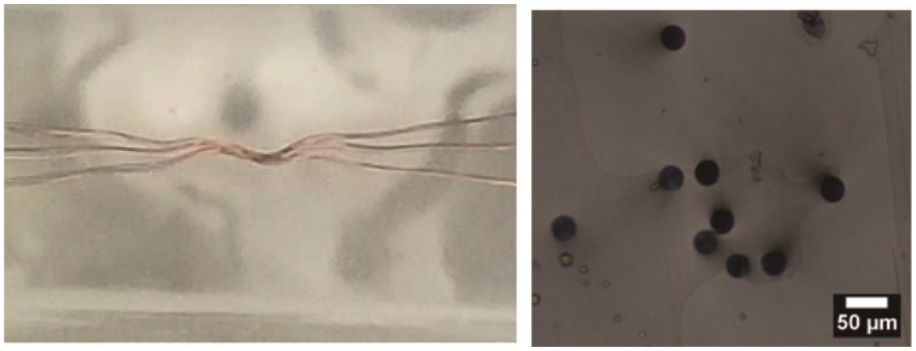

Fig. S5. Deformation of thin wires induced by PDMS shrinkage during curing. (Left) Optical micrograph of a piano wire array embedded in a PDMS block after curing, showing lateral deformation of the wires. (Right) Scanning electron microscopy (SEM) image of the resulting micronozzle array after wire removal and sectioning, exhibiting misalignment of apertures caused by wire displacement during curing.

Simulation of microfluidic flow confinement

The flow field induced by the micronozzle array was evaluated using three-dimensional numerical simulations performed with COMSOL Multiphysics (version 6.1). A single injection–aspiration nozzle pair was modeled to examine fundamental flow confinement behavior under laminar flow conditions (Fig. S6).

The simulation geometry consisted of two circular microchannels representing the injection and aspiration micronozzles. The channel diameter was set to 35 µm, and the center-to-center distance between the two channels was 84.5 µm, corresponding to the experimentally measured dimensions of the fabricated device. The computational domain included the surrounding fluid volume to capture open-space flow confinement.

Water was used as the working fluid and modeled as an incompressible Newtonian fluid with standard physical properties at room temperature. Steady-state laminar flow conditions were assumed. The volumetric flow rates were set to 0.2 µL min^{-1} for injection and 0.4 µL min^{-1} for aspiration, matching the experimental conditions used in the flow confinement experiments. No-slip boundary conditions were applied at all solid–fluid interfaces, and pressure was set to zero at the outer boundaries of the computational domain.

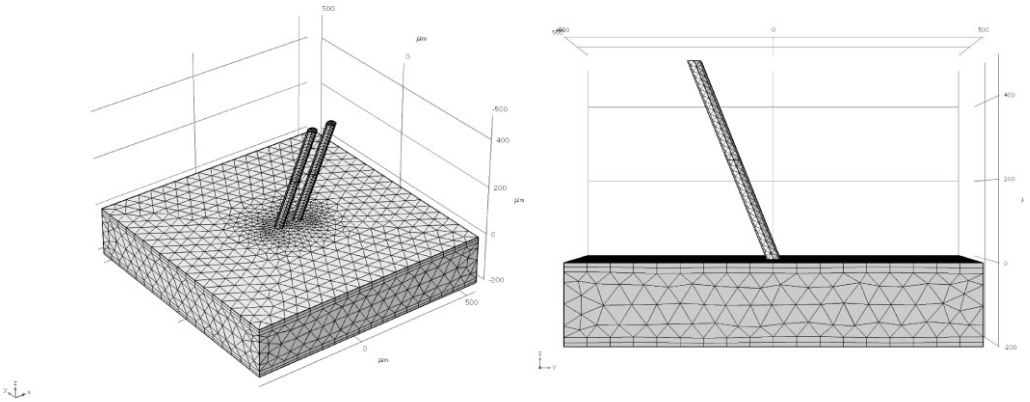

Fig. S6. Three-dimensional simulation model for hydrodynamic flow confinement using a micronozzle array device. Two circular microchannels represent the injection and aspiration micronozzles (diameter: 35 μm; center-to-center spacing: 84.5 μm). The model was used to evaluate flow confinement behavior under laminar flow conditions corresponding to the experimental setup.